

Research Paper

Comparison of Moving Average and Differential Operation for Wheeze Detection in Spectrograms

Meng-Lun HSUEH^{(1)*}, Jin-Peng CHEN⁽²⁾, Bing-Yuh LU⁽²⁾, Huey-Dong WU⁽³⁾, Pei-Yi LIU⁽²⁾

⁽¹⁾ *Graduate Institute of Intelligent Robotics, Hwa Hsia University of Technology*
New Taipei City, Taiwan

⁽²⁾ *Faculty of Automation, Guangdong University of Petrochemical Technology*
Guangdong, China

⁽³⁾ *Department of Integrated Diagnostics and Therapeutics, National Taiwan University Hospital*
Taipei, Taiwan

*Corresponding Author e-mail: elic@go.hwh.edu.tw

(received March 8, 2021; accepted May 13, 2022)

A moving average (MA) is a commonly used noise reduction method in signal processing. Several studies on wheeze auscultation have used MA analysis for preprocessing. The present study compared the performance of MA analysis with that of differential operation (DO) by observing the produced spectrograms. These signal preprocessing methods are not only applicable to wheeze signals but also to signals produced by systems such as machines, cars, and flows. Accordingly, this comparison is relevant in various fields. The results revealed that DO increased the signal power intensity of episodes in the spectrograms by more than 10 dB in terms of the signal-to-noise ratio (SNR). A mathematical analysis of relevant equations demonstrated that DO could identify high-frequency episodes in an input signal. Compared with a two-dimensional Laplacian operation, the DO method is easier to implement and could be used in other studies on acoustic signal processing. DO achieved high performance not only in denoising but also in enhancing wheeze signal features. The spectrograms revealed episodes at the fourth or even fifth harmonics; thus, DO can identify high-frequency episodes. In conclusion, MA reduces noise and DO enhances episodes in the high-frequency range; combining these methods enables efficient signal preprocessing for spectrograms.

Keywords: differential operation; moving average; signal; lung sound; wheeze.



Copyright © 2022 M.-L. Hsueh et al.
This is an open-access article distributed under the terms of the Creative Commons Attribution-ShareAlike 4.0 International (CC BY-SA 4.0 <https://creativecommons.org/licenses/by-sa/4.0/>) which permits use, distribution, and reproduction in any medium, provided that the article is properly cited, the use is non-commercial, and no modifications or adaptations are made.

1. Introduction

Many illnesses induce changes in breathing. These changes can be detected by recording lung sounds. Lung sound auscultation is thus critical. Currently, COVID-19, a form of viral pneumonia, is one of the main causes of death globally (NGUYEN *et al.*, 2021). Consequently, lung sound auscultation is a crucial process for physicians to detect abnormal breathing. A computer-aided lung sound analysis is an accurate method for facilitating auscultation. One commonly applied method of computer-aided lung sound analysis entails visualizing the lung sounds with a spectrogram and subsequently performing an analysis (FRAIWAN

et al., 2021; KUMAR *et al.*, 2021; LANG *et al.*, 2021; LI *et al.*, 2021; LU *et al.*, 2021).

A spectrogram of a signal over time at various frequencies displays power intensities and their distributions. Spectrograms visually represent the strength (or “loudness”) of a signal. In medical auscultation, spectrograms have been increasingly used to analyze the frequency of continuous lung sound signals to identify and characterize abnormal respiration.

A moving average (MA) is a commonly used technique for preprocessing biomedical signals (SOVIJÄRVI *et al.*, 2000; CHARBONNEAU *et al.*, 2000; TABATA *et al.*, 2018; TAPLIDOU, HADJILEONTIADIS, 2007; BERTRAN *et al.*, 2019). MA operates as an effective low-pass

filter or band-pass filter that reduces high-frequency noise (HASHEMI *et al.*, 2011; SOVIJÄRVI *et al.*, 2000). However, low-frequency signal components in a spectrogram can cause noise, hindering signal analysis for wheeze detection (GAVRIELY *et al.*, 1984). A key feature of a wheeze is nonideal harmonic tones (JEERU, 2021; COMAJUNCOSAS, 2010); whether MA can enhance this feature is unknown because the noise in wheeze signals is random. Therefore, spectrogram examination is necessary to identify these tones (LI, HONG, 2015; MENDES *et al.*, 2015). In contrast to MA analysis, differential operation (DO) for signal analysis operates as a high-pass filter. Specifically, DO reduces the low-frequency components of a signal (DE CHEVEIGNÉ, NELKEN, 2019) and could thus enhance wheeze signal features in a spectrogram (BAE *et al.*, 2021; TAPLIDOU *et al.*, 2003).

Accordingly, this study compared the performance of MA analysis, DO, and their combination for capturing wheeze features in spectrograms. Notably, signal preprocessing technology is crucial not only for bioelectric signals but also for signals produced by systems such as machines, cars, and flows. Therefore, a comparison of the performance of MA- and DO-based signal preprocessing methods is applicable to numerous domains.

2. Methods

In MA analysis, the mean value within a signal window can be derived as follows:

$$\bar{x}[n] = \frac{1}{N} \sum_n^{n+N-1} x[n], \quad (1)$$

where $\bar{x}[n]$ is the mean of $x[n]$ to $x[n + N - 1]$, with $n = 1, 2, \dots, 3$ until the end point of the signal. N is the number of window points. In this study, N was set to 3 in accordance with the procedures described by other studies (TABATA *et al.*, 2018; TAPLIDOU, HADJILEONTIADIS, 2007).

Assuming that $x(t)$ is a signal, the first finite difference (DO) of $x(t)$ can be written as follows:

$$\Delta x(t) = \frac{x(t+h) - x(t)}{h}, \quad (2)$$

where Δ is the difference operator, t is time, and h is the interval between $x(t)$ and $x(t+h)$ for a digitally sampled signal $h = 1/f_s$, where f_s is the sampling frequency (WANG *et al.*, 2020).

The element $x[n]$ at the time point n in a spectrogram can be defined as follows (HAYKIN, VAN VEEN, 1998):

$$|X_\eta[j\Omega]|^2 = \left| \sum_{-\infty}^{\infty} x[n] w^*[n-\eta] e^{-j\Omega n} \right|^2, \quad (3)$$

where $w^*(n-\eta)$ is a window function, which is typically a function of real numbers. Therefore, $w^*(n-\eta)e^{-j\Omega n}$ represents an envelope function that causes a time shift of η with a sine wave and a cosine wave. Furthermore, $e^{-j\Omega n}$ is a phasor operator, which is the same as that in the discrete fast Fourier transform (FFT). A spectrogram typically presents the relationship of the magnitude (in dB) of the time-independent discrete Fourier transform with time. In this study, the number of frames for the short FFT was set to 128, and the number of nonoverlapping points was set to 126. Additionally, the study used four input wheeze signals to create spectrograms: an original, unprocessed wheeze signal (OS), a signal processed through DO (DS), a signal processed through the MA method (MS), and a signal processed through a combination of DO and the MA method (DMS). The sampling frequency of the explored signals was determined to be 5512.5 Hz. The computation was executed in the MATLAB R2016a (MathWorks, USA) development environment.

3. Results

To compare the performance of the MA and DO methods, the spectrograms were created for various signals and used for analysis. Figure 1 displays the spectrograms created for the four input signals:

- 1a presents the OS in the time domain; the x -axis represents time, and the y -axis represents amplitude.
- 1b shows the DS in the time domain.
- 1c demonstrates the spectrogram of the OS, indicating eight distinct episodes; the frequency bands of these episodes are at approximately 400 and 800 Hz.
- 1d presents the spectrogram of the DS, revealing 16 episodes with frequency bands at approximately 400, 800, 1200, and 1600 Hz; as the episodes at 1600 Hz could not be distinguished, they are indicated by arrows in the figure.
- 1e shows the MS.
- 1f displays the DMS.
- 1g presents the spectrogram of the MS, revealing eight clear episodes with frequency bands at approximately 400 and 800 Hz.
- 1h demonstrates the spectrogram of the DMS, indicating 12 visible episodes with frequency bands at approximately 400, 800, and 1200 Hz.

Regarding the amelioration of high-frequency noise in the signals, the combination of DO and MA analysis resulted in the best denoising performance. The spectrogram presented in Fig. 1h reveals lower power levels in the high-frequency bands. However, the spectrogram in Fig. 1d exhibits lower power levels in these bands. Accordingly, the DO process also exhibited acceptable

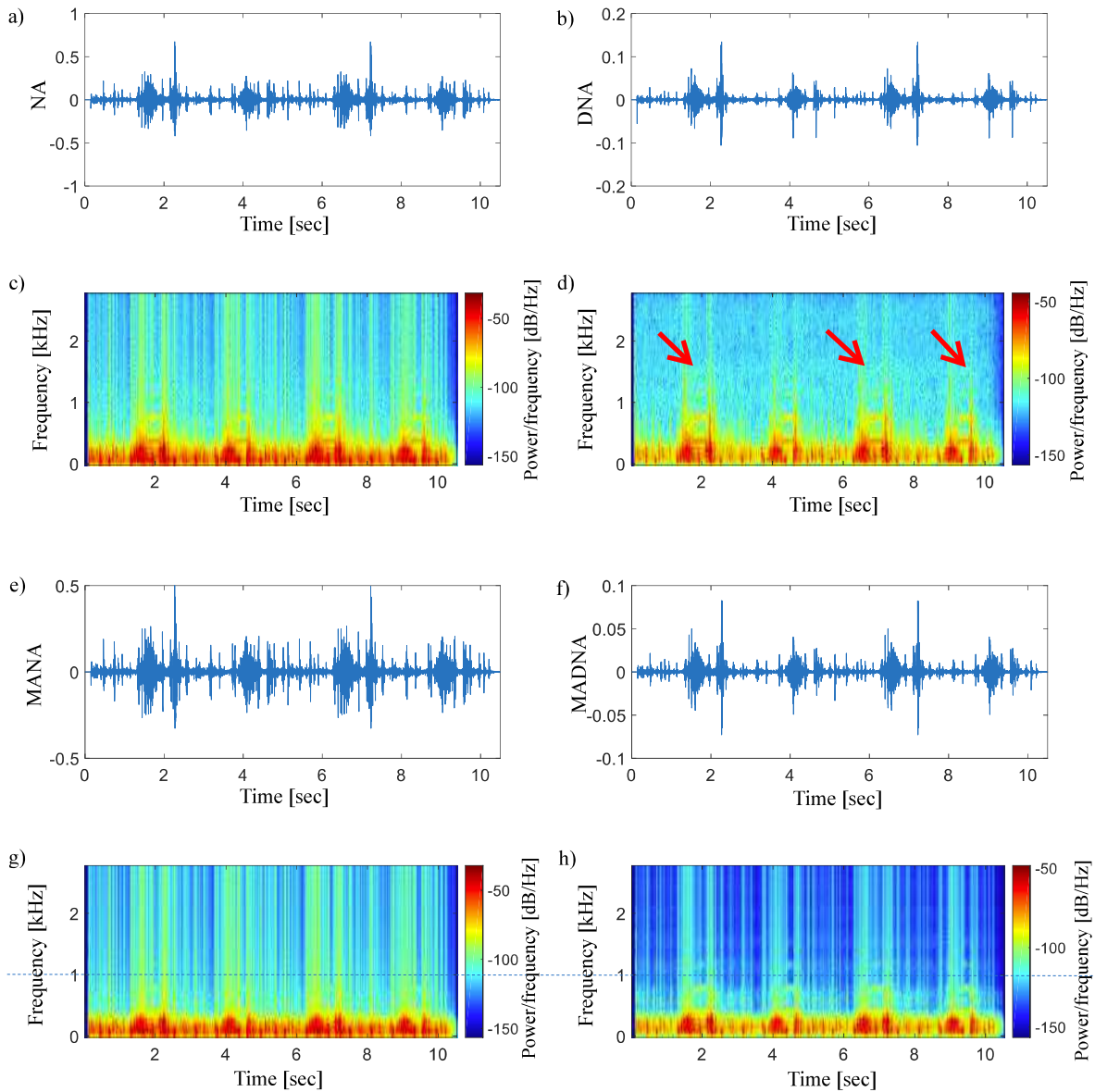


Fig. 1. a) OS, b) DS, c) spectrogram of OS, d) spectrogram of DS, e) MS, f) DMS, g) spectrogram of MS, h) spectrogram of DMS. The dashed line is at 1 kHz. Episodes above the dashed line are observable in d) and h), indicating that DO can detect episodes with high-frequency components.

denoising performance levels. The dashed line indicates 1 kHz. The episodes above the dashed line are observable in Fig. 1d and 1h, revealing the performance of DO in detecting episodes with high-frequency components.

4. Discussion

DO is effective as a high-pass filter. This is supported by the finding of the present study that DO enhanced the high-frequency episodes at 1200 and 1600 Hz (Fig. 1d). Similarly, numerous researchers have employed spectrograms to enhance episodes for wheeze detection (LIN *et al.*, 2015; TAPLIDOU *et al.*,

2003; MENDES *et al.*, 2015). DO enhances such episodes, thus increasing the performance of algorithms used to detect these episodes. Nevertheless, this study notably revealed that the fourth harmonic episodes observed at approximately 1600 Hz were undistinguished after DO in the corresponding spectrogram (Fig. 1d).

MA analysis can reduce high-frequency noise. Accordingly, the power intensity of high-frequency episodes can be averaged using MA analysis. This study revealed that the episodes observed at approximately 1200 Hz in the spectrogram (Fig. 1h) were less distinguished than those observed in the spectrogram (Fig. 1d). Furthermore, the episodes observed at 1600 Hz almost completely disappear in the spectrogram. Signal-to-noise ratio (SNR) calculations were

performed, and the results (Jet bar in the figures) revealed that the SNRs of the high-frequency episodes at 1200 and 1600 Hz in the spectrogram shown in Fig. 1d were greater than 20 dB, but those of the episodes in the spectrogram shown in Fig. 1h were less than 10 dB. Therefore, in terms of SNR, DO outperformed the DO-MA combination; specifically, the SNR for DO exceeded that for the combination by 10 dB.

Conceptually, if Eq. (2) is substituted into Eq. (3), the spectrogram of $\Delta x[n]$ can be expressed as follows:

$$f_s |\Delta X_\eta[j\Omega]|^2 = f_s \left| \sum_{-\infty}^{\infty} (x[n] - x[n-1])w^*[n-\eta]e^{-j\Omega n} \right|^2,$$

i.e.

$$|\Delta X_\eta[j\Omega]|^2 = |X_\eta[j\Omega]|^2 - \left| \sum_{-\infty}^{\infty} x[n-1]w^*[n-\eta]e^{-j\Omega n} \right|^2. \quad (4)$$

If $N = n - 1$, we obtain the following:

$$|\Delta X_\eta[j\Omega]|^2 = |X_\eta[j\Omega]|^2 - \left| \sum_{-\infty}^{\infty} x[N]w^*[N-(\eta-1)]e^{-j\Omega(N+1)} \right|^2. \quad (5)$$

Replacing N with n yields the following:

$$|\Delta X_\eta[j\Omega]|^2 = |X_\eta[j\Omega]|^2 - \left| \sum_{-\infty}^{\infty} x[n]w^*[n-(\eta-1)]e^{-j\Omega(n+1)} \right|^2, \quad (6)$$

therefore:

$$|\Delta X_\eta[j\Omega]|^2 = |X_\eta[j\Omega]|^2 - |e^{-j\Omega} X_{\eta-1}[j\Omega]|^2. \quad (7)$$

Equation (7) indicates that the spectrogram of $x'[n]$ is the difference between $|X_\eta[j\Omega]|^2$ and its phase delay with the adjusted window function. Therefore, the spectrogram of $x'[n]$ is similar to that of $x[n]$.

However, changes in the spectrogram of processed signals can be observed through the formulas theoretically. Accordingly, Eq. (3) can be rewritten as follows:

$$|X_\eta[j\Omega]|^2 = \left| \sum_{-\infty}^{\infty} x_\eta[n]e^{-j\Omega n} \right|^2, \quad (8)$$

that is:

$$x_\eta[n] = x[n]w^*[n-\eta]. \quad (9)$$

After applying DO, we obtain the following:

$$\Delta x_\eta[n] = \Delta x[n]w^*[n-\eta] + x[n]\Delta w^*[n-\eta], \quad (10)$$

therefore:

$$\Delta x[n]w^*[n-\eta] = \Delta x_\tau[n] - x[n]\Delta w^*[n-\eta]. \quad (11)$$

The spectrogram of $\Delta x[n]$ can be expressed as follows:

$$|\Delta X_\eta[j\Omega]|^2 = \left| \sum_{-\infty}^{\infty} \Delta x[n]w^*[n-\eta]e^{-j\Omega n} \right|^2, \quad (12)$$

that is:

$$\left| \sum_{-\infty}^{\infty} (\Delta x_\tau[n] - x[n]\Delta w^*[n-\eta])e^{-j\Omega n} \right|^2 = |X_\eta[j\Omega]|^2 - \left| \sum_{-\infty}^{\infty} x[n]\Delta w^*[n-\eta]e^{-j\Omega n} \right|^2. \quad (13)$$

Notably, all the terms of $(\Delta x_\tau[n] - x[n]\Delta w^*[n-\eta])$ are in the real part. The window function is typically uniform, that is:

$$\omega^*[n-\eta] = (u[n] - u[n-\eta])^*, \quad (14)$$

therefore:

$$\Delta \omega^*[n-\eta] = (\delta[n] - \delta[n-\eta])^*. \quad (15)$$

Substituting Eq. (15) into Eq. (13) yields the following:

$$|\Delta X_\eta[j\Omega]|^2 = |X_\eta[j\Omega]|^2 - |(1 - e^{-j\Omega\eta})X_0[j\Omega]|^2. \quad (16)$$

The right side of Eq. (16) is easily interpreted because $|X_0[j\Omega]|^2$ indicates the spectrogram of $x[n]$ without the window function. Considering the signal originality, $|X_0[j\Omega]|^2$ more clearly reveals the characteristics of a signal in the frequency domain. Equation (16) indicates that the spectrogram of $\Delta x[n]$ is the difference between the spectrogram of $x[n]$ and the phase-changed original spectrogram of $x[n]$ without the window function. Therefore, Eq. (16) indicates the following properties of the processed signals:

- 1) The power intensities in Fig. 1d are shown to be lower than those in Fig. 1c. This was determined to influence the presentation of a larger range of power intensities in the spectrogram. The change in the power intensity resulted in the enhancement of higher-frequency episodes.
- 2) $|X_0[j\Omega]|^2$ represents the spectrogram of $x[n]$ without the window function; thus, $|X_0[j\Omega]|^2$ is not as smooth as $|X_\eta[j\Omega]|^2$. Therefore, the frequency components are clearer in $|X_0[j\Omega]|^2$. Episodes represent the harmonics for specific durations. Therefore, the frequency components of episodes should be enhanced in $|X_0[j\Omega]|^2$. This thus explains the higher-frequency episodes observable in Fig. 1d in this study.

Wheeze sounds produce a more harmonic signal than do other lung sounds. This thus explains why the DS in this study was similar to the OS. Accordingly, DO has superior performance in episode detection in wheeze spectrograms.

In pattern recognition, edge detection is commonly used for enhancing episodes in wheeze spectrograms. Edge detection entails the use of a two-dimensional Laplacian operation to scan an image. Compared with a two-dimensional Laplacian operation, DO method applied in this study is easier to implemented and could be used in other studies on acoustic signal processing.

5. Conclusions

MA analysis is a commonly used preprocessing method for reducing high-frequency noise for wheeze detection. This study compared MA analysis with DO to determine its advantages and disadvantages. On the basis of the study results, we propose that DO is instead used for signal preprocessing in wheeze detection. According to Eq. (16), the reduction of the total power intensity are relatively elevated the power intensity of the specific higher frequency episodes. Furthermore, $|X_0[j\Omega]|^2$ is not as smooth as $|X_\eta[j\Omega]|^2$. Therefore, the frequency components are clearer in $|X_0[j\Omega]|^2$ and the higher-frequency episodes are also enhanced.

DO can improve the performance of other algorithms for detecting episodes in spectrograms. Specifically, DO can help identify high-frequency episodes. This is supported by this study's finding that the episodes could be observed at approximately 1600 Hz in the spectrogram shown in Fig. 1d.

The spectrogram in Fig. 1h has the highest SNR of the four spectrograms, indicating the advantages of combining MA and DO. In the high-frequency range, using the MA reduces noise, and employing DO enhances episodes. Employing a combination of MA and DO is thus an efficient method for signal preprocessing.

Notably, preprocessing technology is crucial not only for bioelectric signals but also for other signals produced by systems such as machines, cars, and flows. Therefore, understanding the relative advantages of MA and DO in preprocessing is critical for numerous applications.

Acknowledgments

This work was supported in part by Guangdong University of Petrochemical Technology, Guangdong, China under project numbers: 702-519244.

References

- BAE W., KIM K., YOON J.-S. (2021), Interrater reliability of spectrogram for detecting wheezing in children, *Pediatrics International*, **64**: e15003, doi: 10.1111/ped.15003.
- BERTRAN K., SÁNCHEZ T., BROCKMANN P.E. (2019), Monitoring asthma during sleep: Methods and techniques, [in:] *Allergy and Sleep*, pp. 175–183, Springer, Cham, doi: 10.1007/978-3-030-14738-9_14.
- CARBONE A., KIYONO K. (2016), Detrending moving average algorithm: Frequency response and scaling performances, *Physical Review E*, **93**(6): 063309, doi: 10.1103/PhysRevE.93.063309.
- CHARBONNEAU G., ADEMOVIC E., CHEETHAM B.M.G., MALMBERG L.P., VANDERSCHOOT J., SOVI-JÄRVI A.R.A. (2000), Basic techniques for respiratory sound analysis, *European Respiratory Review*, **10**(77): 625–635.
- COMAJUNCOSAS J.M. (2009), *Expressive Breath Modeling*, Master Thesis, Department of Information and Communication Technologies, Universitat Pompeu Fabra, Barcelona.
- DE CHEVEIGNÉ A., NELKEN I. (2019), Filters: when, why, and how (not) to use them, *Neuron*, **102**(2): 280–293, doi: 10.1016/j.neuron.2019.02.039.
- FRAIWAN L., HASSANIN O., FRAIWAN M., KHASSAWNEH B., IBNIAN A.M., ALKHODARI M. (2021), Automatic identification of respiratory diseases from stethoscopic lung sound signals using ensemble classifiers, *Biocybernetics and Biomedical Engineering*, **41**(1): 1–14, doi: 10.1016/j.bbe.2020.11.003.
- GAVRIELY N., PALTI Y., ALROY G., GROTEBERG J.B. (1984), Measurement and theory of wheezing breath sounds, *Journal of Applied Physiology*, **57**(2): 481–492, doi: 10.1152/jappl.1984.57.2.481.
- HASHEMI A., ARABALIBIEK H., AGIN K. (2011), Classification of wheeze sounds using wavelets and neural networks, [in:] *2011 International Conference on Biomedical Engineering and Technology*, pp. 127–131, Singapore.
- HAYKIN S., VAN VEEN B. (1998), *Signals and Systems*, pp. 72–87, Wiley, New York.
- JEERU S. (2020), *Wheezing sound source separation applied to single channel respiratory audio mixtures*, Master Thesis, Department of Telecommunication Engineering, Universidad de Jaén, <https://hdl.handle.net/10953.1/13601>.
- KUMAR A., ABHISHEK K., CHAKRABORTY C., KRYVINSKA N. (2021), Deep learning and internet of things based lung ailment recognition through coughing spectrograms, *IEEE Access*, **9**: 95938–95948, doi: 10.1109/ACCESS.2021.3094132.
- LANG R., FAN Y., LIU G., LIU G. (2021), Analysis of unlabeled lung sound samples using semi-supervised convolutional neural networks, *Applied Mathematics and Computation*, **411**: 126511, doi: 10.1016/j.amc.2021.126511.
- LI J. *et al.* (2021), LungAttn: advanced lung sound classification using attention mechanism with dual TQWT and triple STFT spectrogram, *Physiological Measurement*, **42**(10): 105006, doi: 10.1088/1361-6579/ac27b9.
- LI J., HONG Y. (2015), Wheeze detection algorithm based on spectrogram analysis, [in:] *2015 8th International Symposium on Computational Intelligence and*

- Design (ISCID)*, pp. 318–322, China, doi: 10.1109/ISCID.2015.310.
16. LIN B.-S., WU H.-D., CHEN S.-J. (2015), Automatic wheezing detection based on signal processing of spectrogram and back-propagation neural network, *Journal of Healthcare Engineering*, **6**(4): 649–672, doi: 10.1260/2040-2295.6.4.649.
 17. LU B.-Y., HSUEH M.-L., WU H.-D. (2021), Transmission Perspective on the Mechanism of Coarse and Fine Crackle Sounds, *Archives of Acoustics*, **46**(2): 289–300, doi: 10.24425/aoa.2021.136583.
 18. MENDES L. *et al.* (2015), Detection of wheezes using their signature in the spectrogram space and musical features, [in:] *2015 37th Annual International Conference of the IEEE Engineering in Medicine and Biology Society (EMBC)*, pp. 5581–5584, doi: 10.1109/EMBC.2015.7319657.
 19. NGUYEN T., PERNKOPF F. (2022), Lung sound classification using co-tuning and stochastic normalization, *IEEE Transactions on Biomedical Engineering (Early Access)*, doi: 10.1109/TBME.2022.3156293.
 20. SOVIJÄRVI A.R.A., DALMASSO F., VANDERSCHOOT J., MALMBERG L.P., RIGHINI G., STONEMAN S.A.T. (2000), Definition of terms for applications of respiratory sounds, *European Respiratory Review*, **10**(77): 597–610.
 21. TABATA H. *et al.* (2018), Changes in the breath sound spectrum during methacholine inhalation in children with asthma, *Respirology*, **23**(2): 168–175, doi: 10.1111/resp.13177.
 22. TAPLIDOU S.A., HADJILEONTIADIS L.J. (2007), Wheeze detection based on time-frequency analysis of breath sounds, *Computers in Biology and Medicine*, **37**(8): 1073–1083, doi: 10.1016/j.compbiomed.2006.09.007.
 23. TAPLIDOU S.A., HADJILEONTIADIS L.J., PENZEL T., GROSS V., PANAS S.M. (2003), WED: An efficient wheezing-episode detector based on breath sounds spectrogram analysis, [in:] *Proceedings of the 25th Annual International Conference of the IEEE Engineering in Medicine and Biology Society (IEEE Cat. No. 03CH37439)*, pp. 2531–2534, doi: 10.1109/IEMBS.2003.1280431.
 24. WANG Y., GUAN X., DU Y., NAN N. (2020), Harmonics based representation in clarinet tone quality evaluation, [in:] *2020 IEEE International Conference on Acoustics, Speech and Signal Processing (ICASSP 2020)*, pp. 766–770, doi: 10.1109/ICASSP40776.2020.9054020.